Supporting Information

Panigrahy et al. 10.1073/pnas.1311565110

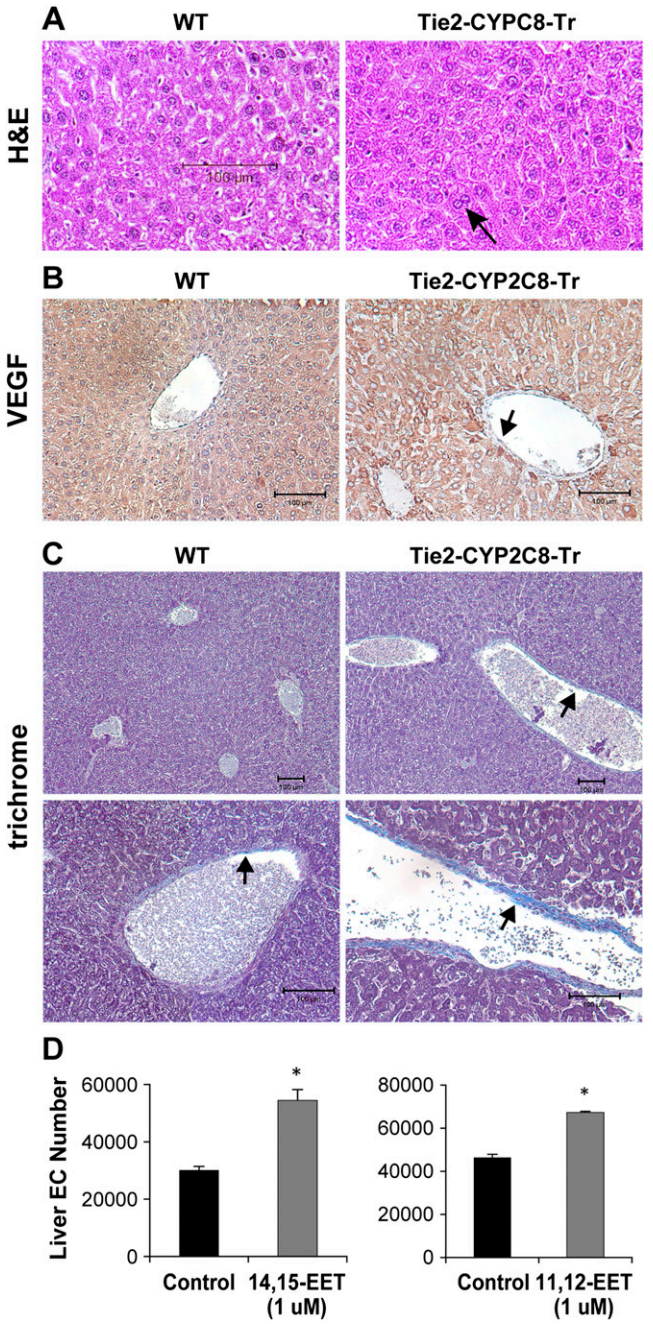

Fig. S1. Endothelial-derived epoxyeicosatrienoic acids (EETs) promote liver, kidney, and lung regeneration. (*A*) Histological analysis of the Tie2-CYP2C8-Tr livers on day 4 after partial hepatectomy revealed increased hepatocyte proliferation characterized by thickening of the hepatocyte cords, multinucleation, and increased nuclear size, features that are typical of dividing cells in a regenerating liver, compared with WT mice. Arrow points to multinucleated hepatocytes in liver from Tie2-CYP2C8-Tr mice. (Scale bar, 100 μm.) (*B*) Immunohistochemistry reveals increased VEGF expression (brown staining) in livers from Tie2-CYP2C8-Tr mice on day 4 after partial hepatectomy compared with WT mice. (Scale bars, 100 μm.) (*C*) Trichrome staining reveals increased collagen deposition (blue staining) in livers from Tie2-CYP2C8-Tr on day 4 after partial hepatectomy compared with WT mice. (Magnification: *Upper*, 10×; *Lower*, 20×.) (Scale bar, 100 μm.) (*D*) The 14,15- and 11,12-EET stimulate liver endothelial cell proliferation. $n = 3$ or 4 per group. $^*P < 0.05$.

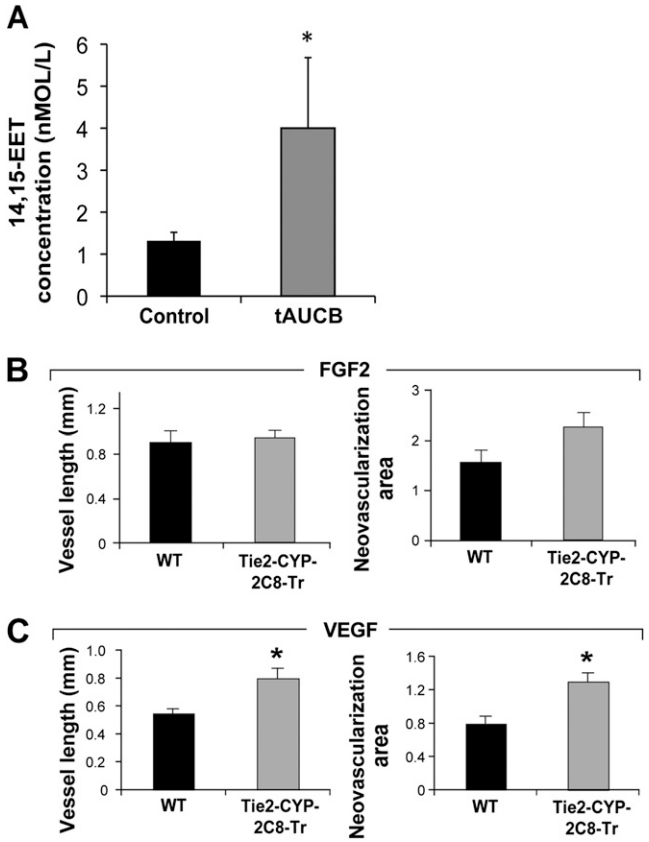

Fig. S2. Pharmacological manipulation of EETs and their action in organ regeneration. (*A*) Systemic administration of the soluble epoxide hydrolase inhibitor (sEHi){trans-4-[4-(3-adamantan-1-ylureido)cyclohexyloxy]-benzoic acid} (*t*AUCB, UC1471) (10 mg·kg^{-1}·d^{-1}) increases 14,15-EET plasma levels. (*B*) FGF-2 (80 ng) induces no significant change in vessel length and neovascularization area in Tie2-CYP2C8-Tr mice vs. WT mice. (*C*) VEGF-induced corneal angiogenesis is increased in Tie2-CYP2C8-Tr mice. VEGF (160 ng) significantly stimulates vessel length and neovascularization area in Tie2-CYP2C8-Tr vs. WT mice. Vessel length and area of neovascularization in Tie2-CYP2C8-Tr and WT mice are represented in bar graphs (mean ± SEM). Neovascularization area is determined on day 6 by the formula $0.2 \times \pi \times$ neovessel length $\times$ clock hours of neovessels ($n = 6$ eyes per group; experiment was performed three times). *$P < 0.05$ vs. WT.

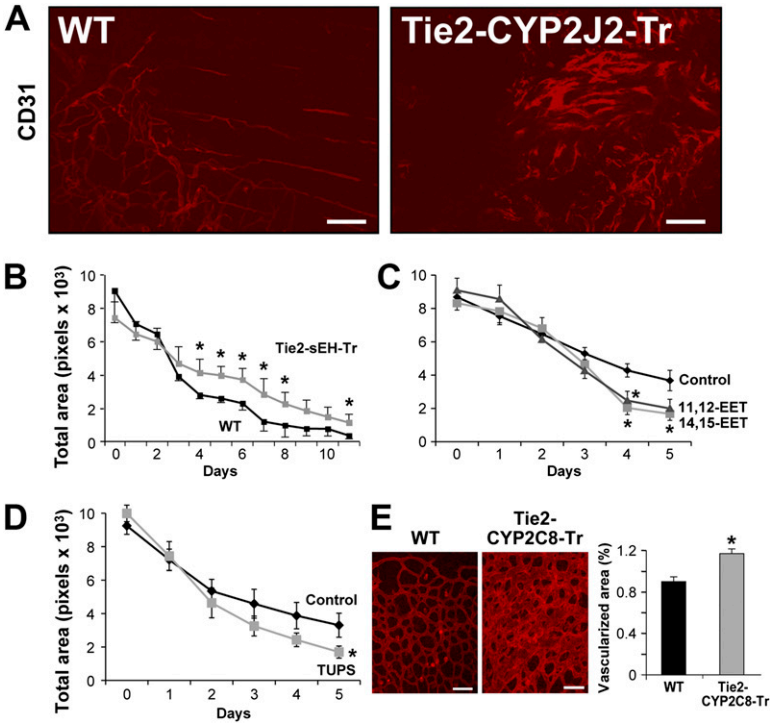

Fig. S3. Endothelial-derived EETs accelerate wound healing and vessel formation. (*A*) Whole-mount immunofluorescent staining (CD31) of wounds on day 10 shows increased vascularization in Tie2-CYP2J2-Tr compared with WT mice. (Scale bars, 100 μm.) (*B*) Time course of delayed wound healing in Tie2-sEH-Tr mice. $n = 8$ wounds per group. $^*P < 0.05$ vs. WT. (*C*) Systemic administration of 14,15- or 11,12-EET (15 $\mu g \cdot kg^{-1} \cdot d^{-1}$) via minipump stimulates wound healing on day 5 compared with vehicle-treated mice. $n = 10$ wounds per group. $^*P < 0.05$ vs. vehicle. (*D*) Topical application of the sEHi 1-(1-methylsulfonyl-piperidin-4-yl)-3-(4-399 trifluoromethoxy-phenyl)-urea (TUPS, UC1709) (0.1% cream) accelerates wound healing on day 5 compared with vehicle-treated mice. $n = 8$–10 wounds per group. $^*P < 0.05$ vs. vehicle. (*E*) Neonatal retinal vessel formation is increased in Tie2-CYP2C8-Tr mice relative to WT mice. Confocal fluorescence micrograph of vessels stained with Alexa 594–isolectin on postnatal day 5. $n = 7$ pups per group. $^*P < 0.05$ vs. WT. (Scale bars, 100 μm.)